NOAA-20 VIIRS Radiometric Band Saturation Evaluation and Comparison with Suomi NPP VIIRS using Global Probability Distribution Function Method

Bin Zhang*[a], Changyong Cao[b], Sirish Uprety[c] and Xi Shao[c]
[a]Earth Resources Technology, Inc, 14401 Sweitzer Lane Suite 300 Laurel, MD 20707;
[b]NOAA/Center for Satellite Applications and Research, College Park, Maryland, USA;
[c]University of Maryland, College Park, MD USA 20740

ABSTRACT

NOAA-20 was successfully launched on Nov. 18, 2017. Intensive radiometric calibration and validation activities for VIIRS onboard NOAA-20 were carried out immediately after the sensor data become available. Several bands of NOAA-20 VIIRS such as M6, and M8 have maximum dynamic range requirements or waivers on the saturation value and require post-launch assessment of the impacts on the L1B (or EDR) products. Since the saturation threshold in data processing is defined as the measured Digital Number (DN) count, the corresponding saturation radiance value in the L1B data product can vary due to detector difference and degradation in the sensor optical throughput. On the other hand, users of L1B data care more about the accuracy of scene-dependent radiance value and the impact of detector saturation on the radiance data. In order to validate the detector saturation level and assess their impacts on the radiance data products, histogram-based Probability Distribution Function (PDF) is derived both at detector level and at band level from the daily global radiance data. With such distribution function, the saturation level in radiance can be identified from the sharp fold-over and cut-off at the high radiance value in the distribution. In addition, the percentage of the affected pixels in the global data can be quantified and the detector performance can be compared. Since NOAA-20 and SNPP are 50 minutes apart in the same orbital plane and have the same equator-crossing time, the probability distribution function method also enables comparison of the radiometric calibration performance between the two sensors. For example, the saturation radiance value for VIIRS M6 on NOAA-20 is ~44.2 (W/m^2-sr-um) on 01/11/2018, which is ~26% lower than that of SNPP VIIRS. Such difference can be traced to the more rapid degradation of rotating telescope assembly mirror reflectance in SNPP VIIRS. In addition to saturation analysis, the PDF method allows us to analyze the VIIRS Day/Night Band (DNB) according to the solar zenith angle range, and the performance of stray light correction can be compared between SNPP and NOAA-20 as well.

Keywords: NOAA-20, VIIRS, Radiometric saturation, Histogram, Probability Distribution Function (PDF)

1. INTRODUCTION

NOAA-20 was successfully launched on Nov. 18, 2017. On board NOAA-20, the Visible Infrared Imaging Radiometer Suite (VIIRS) has the same design as VIIRS onboard Suomi-NPP which has the heritage of MODIS, AVHRR and SeaWIFs. It has 14 Reflective Solar Bands (RSB), 7 thermal emissive bands and one Day/Night Band (DNB), covering a spectra range of 0.41-12.0 um [1]. With different spatial resolution, the 16 moderate resolution bands (M bands M1-M16) have spatial resolution of 750 m near the nadir and the 5 imagery bands (I bands I1-I5) have spatial resolution of 375 m. Products from VIIRS observation are being used to monitor the atmosphere, Ocean, Land and Cryosphere for climate change and short-term weather study and forecasts. Each band has specific stability and calibration requirement in design before launch, and these requirements are to be met in the pre-launch test and post-launch validation. The high spatial resolution and the specific requirements for these spectral bands need to be satisfied to generate high quality operational and scientific data products [2].

VIIRS radiometric calibration has specific requirements in the observed radiance/brightness temperature of dynamic range, signal to noise ratio (SNR) and radiometric accuracy, which are separately defined for each band of RSB, TEB and DNB [2]. The dynamic range specification for each band includes the lower and upper limits of measured radiance/brightness temperature (L_{min}/T_{min} and L_{max}/T_{max}), out of which the observed radiance (or BT) pixels are labeled as bad quality data (do not meet the dynamic range specifications). For example, for NOAA-20, the dynamic range is 5.3/41 W/m^2-sr-um (L_{min}/L_{max}) for band M6, 3.5/164.9 for M8, 3e^{-9}/0.02 W/sr-cm^2 for DNB. The accuracy of radiance

Earth Observing Systems XXIII, edited by James J. Butler, Xiaoxiong (Jack) Xiong, Xingfa Gu, Proc. of SPIE Vol. 10764, 107641Q · © 2018 SPIE · CCC code: 0277-786X/18/$18 · doi: 10.1117/12.2321971

within the dynamic range limits is generally 2% for RSB bands. The SNRs at the typical radiance (L_{typ}) needs to be higher than the specified values to be good quality data. Most of these specific requirements of NOAA-20 are very close to or the same as that of SNPP, but there are some minor differences due to the design differences, such as Relative Spectral Response Functions (RSR) differences. The SDR products at provisional maturity level needs to meet these requirements and specs. For longterm, each band has its own stability requirement, which is necessary especially for climate studies.

Based on lessons learned from SNPP, some bands do have issues in meeting these requirements during either pre-launch test [3] or post launch validation [4]. Due to the electrical design, most of the bands saturate when observing very high scene radiances. A major concern was that, for some bands, the saturation occurs at a level less than L_{max}. For some bands, those scene radiances higher than the saturated value in fact decreases as the scene radiance increases [4]. This phenomenon is called radiance rollover or fold-over, such as band M6. Those erroneous radiances can be even recorded much lower than saturated value and wrongly labeled as good quality in the SDR products because they are within the dynamic range (less than L_{max}). With additional work, those pixels are eventually flagged out in the later SDR products [4]. The saturation radiance less than maximum dynamic range mostly occurs for RSB/SWIR bands from M5 to M11. These can cause problems for Environment Data Record (EDR) users in the early SNPP products and mitigations on EDR levels are needed to solve them. At the SDR level, a correction algorithm has been proposed to flag out these rollover pixels for M6 [4]. Other bands have performance waiver to relieve the maximum dynamic range requirement. However, over time after launch, there exists the RTA minor degradation due to UV induced darkening [4]. The degradation causes the light intensity received by the focal plane actually decreases and hence the saturated radiance values would increase along with time, eventually exceeds the L_{max} several years postlaunch for SNPP.

For NOAA-20 VIIRS, pre-launch test showed radiance of most of bands meet radiance dynamic range specification, and generally the saturation values are higher than L_{max} with margins more than about 10%, and slightly different from SNPP. Exceptions are for M8 and M9, where the saturated radiance is only 0.72 (M8) and 0.94 (M9) of Lmax. The saturation radiance for NOAA-20 VIIRS is not expected to change as much as SNPP. Considering the dynamic range, the saturation values and rollover, waivers have been given to some bands such as M8. Although M6 has radiance rollover, it did not require a waiver partly because only low radiances are needed for EDR products.

For DNB, the dynamic range spans seven orders of magnitudes since it needs to observe from night light (such as aurora, city lights etc.) to full day light. It has three dynamic range segments, corresponding to low/middle/high gain stage. One of the major issues in DNB observation is the stray light effects. When the sensor is in the terminator zone, stray light in the DNB can enter the focal plane at specific satellite solar zenith angles (SZA), even at night. The contamination gives false radiances which violates the requirements. Thus waiver mitigation for DNB is proposed to remove stray light effects at SDR level, which requires code change and look up table updates for both SNPP and NOAA-20 VIIRS post launch. The VIIRS DNB data from SNPP and NOAA-20 are slightly different, since NOAA-20 DNB has an extended frame zone, which make the stray light correction algorithm different from that of SNPP.

Monitoring of the on-orbit performance for each VIIRS band is carried on once the nadir door was opened and SDR data were produced. One simple but important CAL/VAL task is to check the dynamic range and saturation/rollover for each band and to compare with prelaunch test results and specific requirements. And long term monitoring of these bands are also needed for degradation to meet the stability requirements. In this study, we used the global Probability Distribution Function (PDF) methods (aka, Histogram) to check the early measurements from recently launched NOAA-20, mainly focusing on the diagnosis of dynamic ranges, band saturation, and comparison with SNPP results, pre-launch measurements and specific requirements.

2. METHODS AND DATA SETS

The histogram or PDF method is very useful for detecting saturation, which shows the probability distribution of the radiance with frequency of occurrences. Usually the saturation shows a cut-off value in the histogram. For each band studied, generally one day of global data sets are used to create the histogram and calculate the statistics. We used the NOAA-20 Level-1B (or SDR) datasets, which can be downloaded from NOAA-CLASS, and also reprocessed SNPP/NOAA-20 datasets which are locally available on super computers of CICS/UMD and GRAVITE/NOAA. For each day there are about 1013 VIIRS granules, each with 48 scans for 16 (M band) or 32 (I band) detectors. The histogram is calculated for all observed radiance of the entire day for the specific band. Some histograms at detector levels are also been calculated since each detector has its own spectral response and hence different radiance values. The

radiance data are binned into 1000 groups with equal intervals from 0 to its detected maximum values and the numbers of radiance values fallen into each group are counted. For DNB, due to its large range in radiances covering several orders of magnitude, logarithm of radiance bins is used for histogram generation. Although VIIRS has 22 bands, in this study, we only focus on the band M6, of which the fold-over radiance led to quality issues in the SDR products, the M8 band, which requires a performance waiver due to saturation, and the DNB band to check the stray-light correction effects. Results for other bands will be discussed later.

3. NOAA-20 VIIRS AND HISTOGRAM COMPARISON WITH SNPP

3.1 VIIRS Bands M6/M8 Dynamic Range, Saturation, and Comparison with SNPP

It has been found that for SNPP VIIRS, when the observed M6 radiance exceeds the saturated value (L_{sat}), the radiance rollover can happen. As a result, pixels with higher scene radiance may instead get smaller radiance values than the L_{sat}, usually with decreasing digital count number [4]. Figure 1 shows the histogram of the NOAA-20 M6 radiance globally on 01/11/2018 overlaid with the same day SNPP radiance distribution globally. Clearly, both SNPP and NOAA-20 bin count numbers stopped increasing abruptly at different radiance levels. NOAA-20 VIIRS M6 radiance reaches the maximum points at 44.2 (W/m^2-sr-um), while the maximum value for SNPP is 59.8 (W/m^2-sr-um). Theoretically, without saturation, we expect the right tail of the histogram curve gradually changed to zero with increasing radiance values and the histogram of SNPP and NOAA-20 should match each other consistently. The difference between these two implies the instrument response difference. The count starts to increase around 35 W/m^2-sr-um for NOAA-20 and

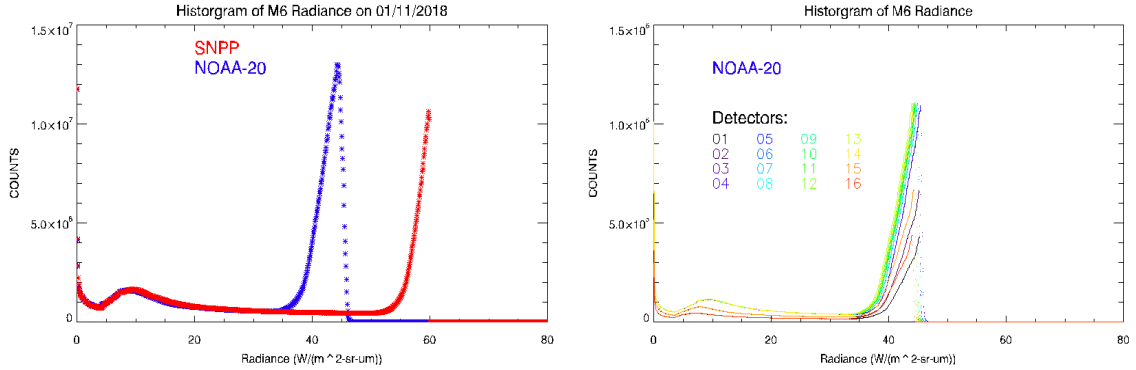

Figure 1 a.) Histogram of VIIRS M6 Radiance on 01/11/2018. Red line is for SNPP, and Blue line is for NOAA-20. b.) Histogram of NOAA-20 VIIRS M6 Radiance on detector level.

the same happens around 52 W/m^2-sr-um for SNPP. Maximum radiance values at the count peak indicating the saturation radiance for both SNPP and NOAA-20, and NOAA has a smaller saturation value. In other words, from about 35 to 44.2 W/m^2-sr-um, most of the scene radiance observed are saturated, and the actual scene radiance should be higher than recorded values. The number of pixels with radiance between 0-35 W/m^2-sr-um is about 36.48% for NOAA-20. The number of pixels with radiance between 0-52 W/m^2-sr-um is about 60.17%. The percentage here represents a rough estimation about how many good pixels for NOAA-20 and SNPP, respectively. With smaller saturation radiance, we do expect the NOAA-20 has less number of good pixels. We also see slight difference in the peak around 10 W/m^2-sr-um. Though histogram can give us a rough estimation of how many pixels are saturated, how to distinct each pixel needs information from other channels. The histogram difference between the SNPP and NOAA-20 is mainly due to the saturation level differences. VIIRS M6 is mainly used for atmosphere correction for ocean color with low radiances and it is also used in aerosol products. The saturated pixels may cause problems and these data were not flagged in the early SNPP and NOAA-20 SDR products in IDPS.

The NOAA-20 and SNPP M6 radiance have both specification of L_{max} value of 41 W/m^2-sr-um. The M6 radiance ratio of L_{sat}/L_{max} is about 1.08, still matches dynamic range requirement, comparable to prelaunch test of 1.16 with a smaller margin.

At detector level, the saturation radiances are slightly different (Figure 1b). For example, detector 3 and 4 have the saturation radiance of 45.51 W/m^2-sr-um while detectors 16 have value of 43.96 W/m^2-sr-um. Therefore at detector level, the NOAA-20 M6 upper limit of the dynamic range is smaller than the saturation radiance for all detectors.

However, similar to the all detector histogram, there is radiance rollover which can be detected for all detectors, showing as the gradually increases of bin count numbers towards saturation value.

In the histogram, the other peak occurs around typical radiance (L_{typ}) of 9.6 W/m^2-sr-um. With different detector, the peak radiances for each detector are different. Basically, the peaks are separated roughly into three groups for NOAA-20, which are related to their RSR differences in NOAA-20 VIIRS.

Scatter plots of global M6 and M7 radiances shows details of information about the saturation at pixel levels (Figure 2). The M6 radiance clearly rolls over once passing its saturation point while the M7 radiance shows a constantly increase

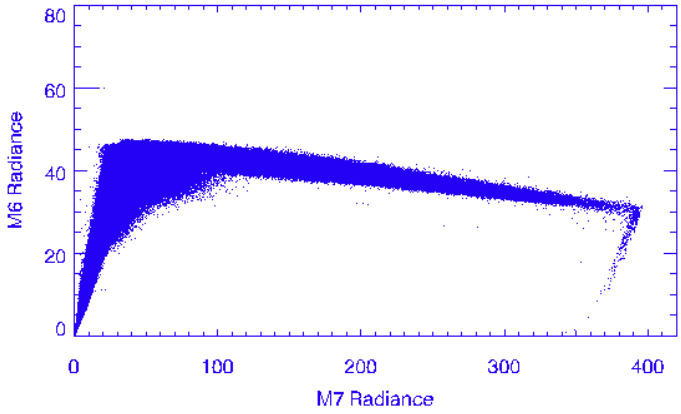

Figure 2 Scatter plot of M6 and M7 radiance of 01/11/2018

until about 390 W/m^2-sr-um. The approximately linear decrease of M6 radiance is in clear contract to M7 radiance exceeding more than about 30 W/m2-sr-um. Also the rollover changes direction after M7 radiance reaches saturation values near 390 W/m^2-sr-um. It is observed that all pixels with M7 radiance value higher than 150 can be regarded as M6 saturated/rollover pixels. However, when M7 radiance exceeds 330 W/m^2-sr-um, the M6 radiance is reduced to below 30 W/m^2-sr-um and even reaches to the Ltyp (9.6 W/m2-sr-um). The M6 accuracy requirement is that 'an accuracy of 2% at 9.6 watt m^{-2} sr^{-1} μm^{-1} for an unpolarized, no contrast scene' [2]. The false radiance at this level certainly does not meet this requirement, and clearly the radiance difference can be easily more than 50% off. Those data need to be flagged with quality issues. From the scatter diagram, the M6 saturated/rollover pixels can be screened out by using the correlation between M6 and M7. In the early NOAA-20 SDR products, the M6 saturated data had not been flagged, and an algorithm has been implemented in IDPS by Wenhui Wang at NOAA/STAR to implement the quality mask flag. The difficulty of flagging the radiance in M6 radiance above 20 may cause problems since there is no clear exact linear relationship between these two channels. However, M6 typical radiance is around 9.6 W/m^2-sr-um. At this radiance level, the data mostly is not contaminated except when M7 radiance is saturated for a few data pixels, which can be easily identified by looking at the M7 radiance values (e.g. greater than 300 W/m^2-sr-um) to determine where these rollover pixels are located.

To assess detector level radiance rollover/saturation impacts on the striping, a daily map of M7 and M6 radiance over mid Atlantic area on 01/11/2018 is analyzed in Fig. 3. From the M7 image, the contrast between clouds and surrounding waters is very sharp, with cloud being bright white and the ocean dark. However, the M6 radiance shows blurred contrast. The bright cloud in M7 radiance map appears dulled grey in M6, indicating lower values than the real radiance and saturated radiance. Also, another feature is the striping. Since the saturation radiance for each detector are different and the rollover values are not the same even with the same scene radiance; this detector level differences caused striping can be as high as 3%. Users of M6 need to be very careful when interpolating the results. The M6 is used in the ocean color and aerosol; most of the useful radiance are around its typical value. The low rollover radiances are mainly from the water leaving clouds. Therefore, once the pixels are flagged, there should be no major impacts on the EDR products when dealing with ocean color and aerosols, with typical radiance at L_{typ}.

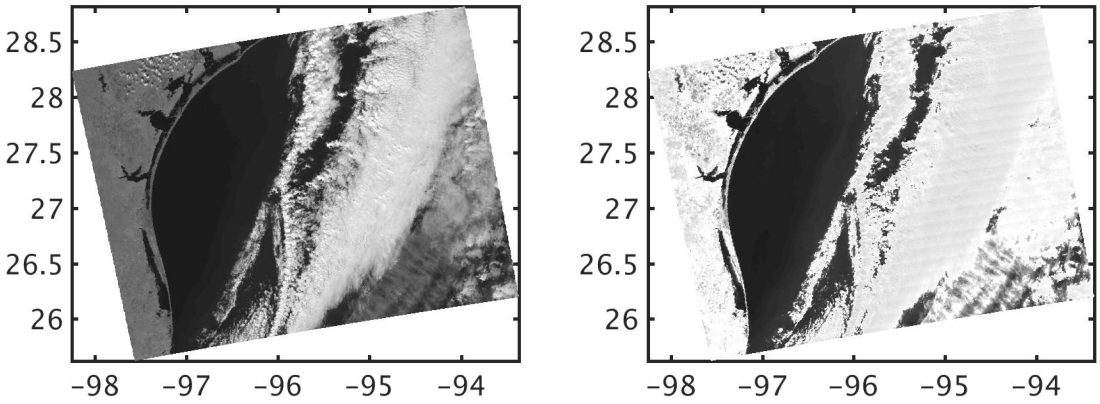

Figure 3 Comparison between M6 and M7 radiance to show the saturation effects

Histogram of VIIRS M8 for both SNPP and NOAA-20 of 01/11/2018 are given in Figure 4. The NPP maximum radiance value is about 196 W/m^2-sr-um and no clear saturation can be detected. But for NOAA-20, there is an abrupt drop of counts around 113 W/m^2-sr-um to 126 W/m^2-sr-um compared to the slowly decreasing of SNPP radiance towards 200 W/m^2-sr-um. The lack of data beyond 126 W/m^2-sr-um of NOAA-20 indicates this band is also saturated: the scene radiance greater than that has been recorded in the SDR dataset with much smaller values. In Fig 4a, there are a few clear small peaks beyond 113 W/m^2-sr-um. This turns out to be caused by different saturation values of different detectors. Without differentiating each detector, it is hard to see if there are any roll-over pixels. Detector level histogram (Fig 4b) indeed shows these spikes are caused by different detectors with different saturation levels. The radiance bin counts increase gradually toward their saturation values, which indicates roll-over too, where the saturated radiance value are rolled over and the count number of lower radiance values increase. However, different from M6, the number of pixels near the saturation levels is very small (less than 0.1%), compared to large amount of M6 roll-over pixels (>50%).

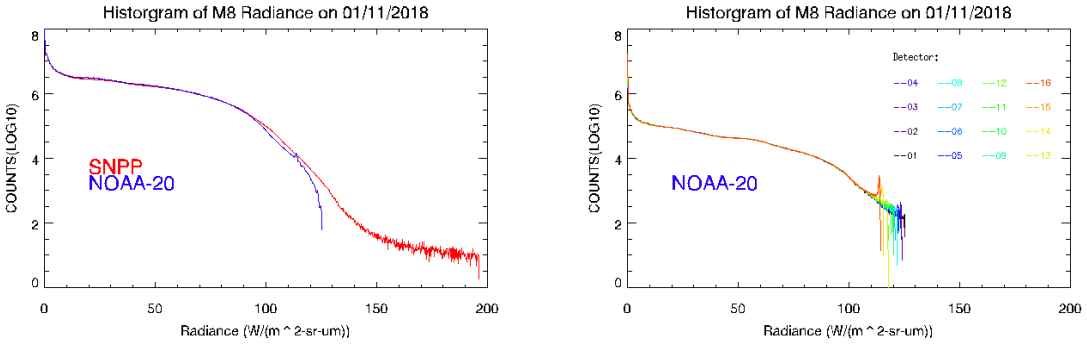

Figure 4 a.) Histogram of M8 Radiance on 01/11/2018. The number counts are on a logarithm scale. The Red line is for SNPP, and blue line is for NOAA-20. B.) Detector level histogram of M8 radiance for NOAA-20.

The NOAA-20 M8 L_{max} is 164.9 W/m^2-sr-um and the saturation has been reported in the prelaunch performance test [1] with the L_{sat}/L_{max} ratio is about 0.72 (118.7 W/m^2-sr-um). Here, at detector level, the smallest saturation radiance among all detectors is 113.7 W/m^2-sr-um for detector 16, the largest is 125.3 W/m^2-sr-um for detector 1, all well below L_{max}, which does not meet the dynamic range requirement. However, M8 does have an instrument performance waiver to relieve the maximum radiance requirement.

M8 data are mainly used for water cloud particle, cloud masks, aerosol optical depth and even night combustion fire detections [7]. The saturation/rollover radiances within the dynamic range have minor to moderate impact on these EDR products and the waiver mitigation is expected to be done on the EDR product level [8].

This study only show results for M6/M8. Other bands also have similar saturation problems, results are not discussed here but will be covered in future work.

3.2 Continuous Monitoring of M6 Saturation using Histogram

The saturation is caused by the limits of the Analog to Digital Converter for the VIIRS bands, which has a dynamic range limit of the digital count number [6]. This maximum digital count limit does not change over the life span. However, the input light received by the band focal plane through the telescope changes with time due to the degradation of the RTA mirror for SNPP even for the same scene radiance [4]. Therefore, the observed maximum saturated radiance, especially for SNPP M6, can be predicted over time due to the degradation of RTA.

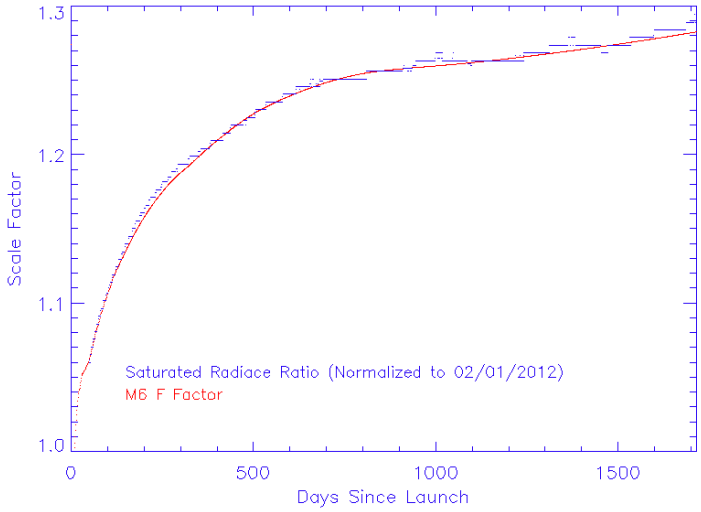

Figure 5 Daily time series of saturated radiance (normalized) of SNPP M6 and F factor from VIIRS Reprocessing

By analyzing daily saturation values, we can monitor the instrument degradation. Fig. 5 shows the normalized daily saturation radiances for SNPP M6 and RTA F factor, which agree well with each other. The saturation radiance of M6 becomes larger and larger with time. This implies the number of rollover pixels falling outside the dynamic range becomes less and less. The RTA degradation of SNPP has led to more frequent update of the F factors to obtain correct radiance. The calibration of the SDR radiance is formulated as in [5]:

$$\overline{L_{ap}(\theta_{ev}, B)} = \frac{F \cdot \sum_0^2 C_i \cdot (DN_{ev} - DN_{sv})^2}{RVS(\theta_{ev}, B)}$$

DN_{ev} is earth view digital count. DN_{sv} is space view digital count, which is quite stable. C_i are the delta-c coefficients, which are determined prelaunch, changing slightly with instrument temperature and response versus scan function (RVS). At saturation, the DN_{ev} reaches maximum and its values hardly change. The term with large uncertainty for SNPP is the F factor, a scaling factor, which needs constant update to account for the RTA degradation. Thus this explains the saturation radiance and F factor relation in the figures above. This gives us an idea of usefulness of the histogram in monitoring the RTA degradation.

The RTA design of NOAA-20 has used a different material to reduce the degradation. Thus we expect to see a relatively flat curve for a long term and it will be closely monitored.

3.3 VIIRS DNB Histogram Analysis

Figure 6a shows the DNB histogram comparison for 01/11/2018 for both SNPP and NOAA-20 during night with local Solar Zenith Angle (SZA) greater than 108°. The NOAA-20 DNB SDR data used here is without stray light correction and SNPP data has stray light correction. Fig 6b shows the DNB radiance histogram for pixels with local SZA greater

than 120 (measurements of these pixels not affected by stray lights). Clearly the difference is mainly caused by the stray light effects. The stray light only occurs at the area with satellite SZA less than 118.4°, based on the satellite height and the Sun position). There is a slight difference in the peaks between NOAA-20 and NPP in Fig 6a, at which NOAA-20 has a smaller radiance ($2.36e^{-10}$ W/sr-cm^2) than the SNPP ($3.19e^{-10}$ W/sr-cm^2). In Fig.6b, NOAA-20 also has slightly smaller peak radiance than NPP. Otherwise, NOAA-20 and NPP agrees well although NOAA-20 histogram is a bit noisy compared to the NPP one which is probably related to the DN0 look up table differences. That day is five days before a new moon. The lunar illumination can be slightly different due to the crossing time differences of the SNPP and the NOAA-20. Also for the same scene, such as city lights, was observed at different local time by SNPP and NOAA-20. All those could be account for the peak radiance difference.

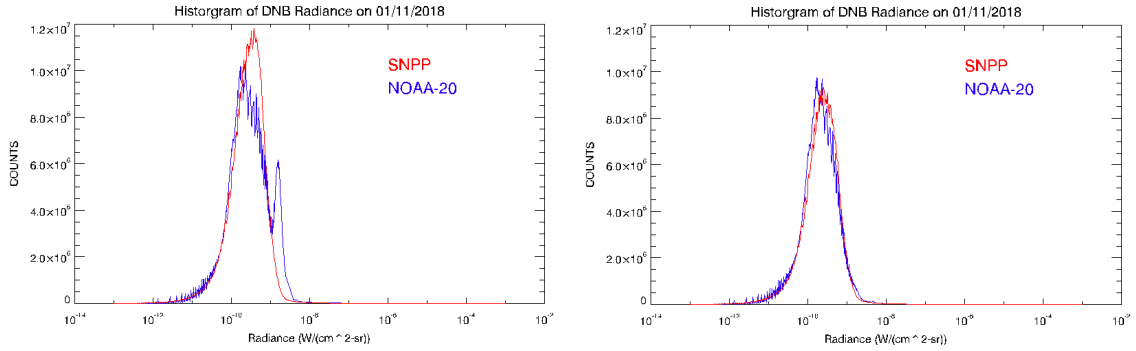

Figure 6 VIIRS DNB Histogram comparison with local SZA greater than 108 (a,left) and with local SZA greater than 120(b, right).

Figure 7 shows the full day DNB radiance histogram of SNPP and NOAA-20 on 06/13/2018, which is a new moon day and the calibration look up table has been updated since Jan 2018 to reduce the negative values in DNB radiance (and hence higher positive radiances, which are usually from air glow) including the new algorithm for stray light correction. That day is new moon day and there was no lunar illumination at night. The daily histogram shows two distinct features at night (left peak) and the day time (right peak). The SNPP and NOAA-20 resembles each other but with minor differences. A few spikes in day time show different surface types, respectively from clouds, land or ocean. The DNB saturates at 0.0047 W/sr-cm^2 at day time. During night, the peak shifted from that for the 01/11/2018 and there is a slight stray light effect around $1.e^{-9}$ W for SNPP, which is likely from stray light residual from the correction algorithm. The shape difference of the night part of the histogram (<1.e-9 W/sr-cm^2) looks quite different for this day, which attributes to the updated DN0 look up table differences, where there are more negative radiance numbers in SNPP than NOAA-20. Note the NOAA-20 histogram is noisier at night than that for SNPP and we used 100 bins instead of 1000 for this scenario, to make histograms look smoother to be compared easily.

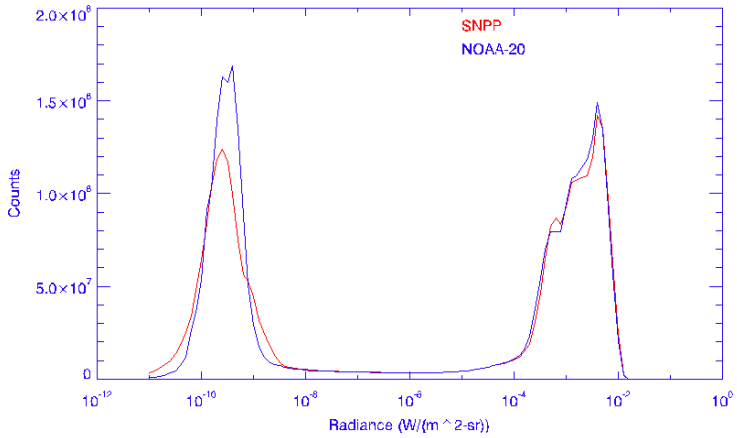

Figure 7 Full day DNB radiance histogram comparison between SNPP and NOAA-20 on 06/13/2018

4. DISCUSSION AND SUMMARY

In this study, the histogram and probability distribution function (PDF) method is used to diagnose the dynamic range, saturation of radiance for Bands M6, M8 and DNB of NOAA-20 VIIRS and compared with SNPP as well as prelaunch tests. From the histogram analysis of 01/11/2018, M6 saturated around 44.2 W/m2-sr-um, which is ~26% lower than that of SNPP VIIRS. Scene radiance exceeding saturation radiance rolled over and therefore are recorded as smaller than the saturation radiance. Since these saturated and rollover radiances are usually less than the maximum dynamic range, the data may be erroneously labeled as good quality in SDR products. The inter-band dependency (M6/M7) can be used to isolate these pixels and flagged these pixels. The detector difference of the saturation/rollover radiance can cause up to about 3% striping. The M8 radiance saturates at radiance level 113.7 W/m2-sr-um for detector 16 and 125.3 W/m2-sr-um for detector 1, which do not meet the L_{max} spec (similar to the prelaunch test results). Also there are a small amount of rollover radiance for M8. However, there is a performance waiver for the M8 maximum dynamic range requirement. At EDR level, the waiver is addressed to reduce the impact on the EDR products. The DNB histogram can be used to indicate different lights scenes, such as Day/Night scenarios, the stray lights, illuminations from different surface type etc. The day time DNB histogram shows saturation, but generally it will not affect the VIIRS DNB Near Constant Contrast (NCC) products with its strong contrast to the low level lights.

We found that in the long term, histogram can be used to monitoring the degradation of the RTA mirror for the bands with radiance saturation, especially for SNPP. It is an indirect measurement of the VIIRS RSB band F factor or radiometer gain.

ACKNOWLEDGMENTS

The manuscript contents are solely the opinions of the authors and do not constitute a statement of policy, decision, or position on behalf of NOAA or the U.S. government.

REFERENCES

[1] Oudrari, H., McIntire, J., Xiong, X., Butler, J., Ji, Q., Schwarting, T., Lee, S. and Efremova, B., JPSS-1 VIIRS Radiometric Characterization and Calibration Based on Pre-Launch Testing. *Remote Sens. 8*, 41 (2016).

[2] JPSS VIIRS ATBD, Joint Polar Satellite System (JPSS) VIIRS Radiometric Calibration Algorithm Theoretical Basis Document (ATBD).

[3] Oudrari, H., McIntire, J., Xiong X., Butler, J. J., Lee, S., Lei, N., Schwarting, T., and Sun J., "Prelaunch Radiometric Characterization and Calibration of the S-NPP VIIRS Sensor." *IEEE Transactions on Geoscience and Remote Sensing* 53: 2195-2210 (2015).

[4] Cao, C., Deluccia, F., Xiong, X., Wolfe, R. and Weng, F., Early On-Orbit Performance of the Visible Infrared Imaging Radiometer Suite Onboard the Suomi National Polar-Orbiting Partnership (S-NPP) Satellite. Geoscience and Remote Sensing, IEEE Transactions on. 52. 1142-1156. 10.1109/TGRS.2013.2247768 (2014).

[5] Datla, R., Shao, X., Cao, C., Wu, X., Comparison of the Calibration Algorithms and SI Traceability of MODIS, VIIRS, GOES, and GOES-R ABI Sensors. *Remote Sens., 8*, 126 (2016).

[6] Madhavan, S., Angal, A., Dodd, J., Sun, J. and Xiong, X.., Analog and digital saturation in the MODIS reflective solar bands. 85101N. 10.1117/12.929998 (2012).

[7] Elvidge, C., Zhizhin, M., Hsu, F.C. and Baugh, K., What is so great about nighttime VIIRS data for the detection and characterization of combustion sources? Proceedings of the Asia-Pacific Advanced Network. 35. 33-48. 10.7125/APAN.35.5 (2014).

[8] Wang, W and Cao C, "J1 VIIRS Waiver Mitigations ", 08/26/2105, https://www.star.nesdis.noaa.gov/star/documents/meetings/2015JPSSAnnual/dayThree/04_Session6a_Wang_J1VIIRSWaiverMitigations.pdf